Luminance enhancement of electroluminescent devices using highly dielectric UV-curable polymer and oxide nanoparticle composite

Seok-Hwan Chung,[1] Seongkyu Song,[1] Kee-Jeong Yang,[2] Soon Moon Jeong,[1] and Byeongdae Choi[1,*]

[1]*Nano & Bio Research Division, Daegu Gyeongbuk Institute of Science and Technology (DGIST), 50-1 Sang-ri, Hyeonpung-myeon, Dalseong-gun, Daegu 711-873, South Korea*
[2]*Energy Research Division, Daegu Gyeongbuk Institute of Science and Technology (DGIST), 50-1 Sang-ri, Hyeonpung-myeon, Dalseong-gun, Daegu 711-873, South Korea*
[*]*bdchoi1@dgist.ac.kr*

Abstract: A flexible hybrid structure electroluminescent (HSEL) device was fabricated from ZnS:Cu phosphor microparticles dispersed in a UV-curable polymer matrix. We observed a maximum luminance of 111 cd/m^2 at 10 kHz and 170 V from a device wherein the mixing ratio between the phosphor particles and highly dielectric polymer binder was 70:30 wt%. Furthermore, by uniformly dispersing highly dielectric BaTiO$_3$ nanoparticles within the polymer matrix, we were able to obtain a luminance of up to 211 cd/m^2 in the HSEL device. Compared to the conventional thermal curing process, this UV process greatly simplifies the fabrication steps by combining phosphors and dielectric materials at room temperature. This process also demonstrates a promising pathway toward creating flexible and printed EL devices in the future.

OCIS codes: (230.0230) Optical devices; (120.2040) Displays; (260.3800) Luminescence; (160.5470) Polymers; (160.4236) Nanomaterials.

References and links

1. S.-I. Park, Y. Xiong, R.-H. Kim, P. Elvikis, M. Meitl, D.-H. Kim, J. Wu, J. Yoon, C.-J. Yu, Z. Liu, Y. Huang, K.-C. Hwang, P. Ferreira, X. Li, K. Choquette, and J. A. Rogers, "Printed assemblies of inorganic light-emitting diodes for deformable and semitransparent displays," Science **325**(5943), 977–981 (2009).
2. M. S. White, M. Kaltenbrunner, E. D. Głowacki, K. Gutnichenko, G. Kettlgruber, I. Graz, S. Aazou, C. Ulbricht, D. A. M. Egbe, M. C. Miron, Z. Major, M. C. Scharber, T. Sekitani, T. Someya, S. Bauer, and N. S. Sariciftci, "Ultrathin, highly flexible and stretchable PLEDs," Nat. Photonics **7**(10), 811–816 (2013).
3. D.-H. Kim, J. Viventi, J. J. Amsden, J. Xiao, L. Vigeland, Y.-S. Kim, J. A. Blanco, B. Panilaitis, E. S. Frechette, D. Contreras, D. L. Kaplan, F. G. Omenetto, Y. Huang, K.-C. Hwang, M. R. Zakin, B. Litt, and J. A. Rogers, "Dissolvable films of silk fibroin for ultrathin conformal bio-integrated electronics," Nat. Mater. **9**(6), 511–517 (2010).
4. K.-I. Park, J. H. Son, G.-T. Hwang, C. K. Jeong, J. Ryu, M. Koo, I. Choi, S. H. Lee, M. Byun, Z. L. Wang, and K. J. Lee, "Highly-efficient, flexible piezoelectric PZT thin film nanogenerator on plastic substrates," Adv. Mater. **26**(16), 2514–2520 (2014).
5. T. I. Kim, Y. H. Jung, J. Song, D. Kim, Y. Li, H. S. Kim, I.-S. Song, J. J. Wierer, H. A. Pao, Y. Huang, and J. A. Rogers, "High-efficiency, microscale GaN light-emitting diodes and their thermal properties on unusual substrates," Small **8**(11), 1643–1649 (2012).
6. H. Kobayashi, K. Ohmi, K. Ichino, and T. Kunimoto, "Research on inorganic electroluminescence – present status," Phys. Status Solidi **205**(1), 11–14 (2008).
7. W. M. Yen, S. Shinoya, and H. Yamamoto, *Fundamentals of Phosphors* (CRC Press, 2007).
8. P. D. Rack and P. H. Holloway, "The structure, device physics, and material properties of thin film electroluminescent displays," Mater. Sci. Eng. **R21**, 171–219 (1997).
9. A. N. Krasnov, "Selection of dielectrics for alternating-current thin-film electroluminescent device," Thin Solid Films **347**(1-2), 1–13 (1999).
10. W. E. Howard, "The importance of insulator properties in a thin-film electroluminescent device," IEEE Trans. Electron. Dev. **24**(7), 903–908 (1977).

11. T. Satoh, N. Nakatsuta, K. Tsuruya, Y. Tabata, T. Tamura, Y. Ichikawa, and H. Tango, "Electrical properties of two-sided luminescence powder-distributed inorganic electroluminescence panels," J. Mater. Sci. Mater. Electron. **18**(S1), 239–242 (2007).
12. M. J. Kim, D. W. Shin, J.-Y. Kim, S. H. Park, I. T. Han, and J. B. Yoo, "The production of a flexible electroluminescent device on polyethylene terephthalate films using transparent conducting carbon nanotube electrode," Carbon **47**(15), 3461–3465 (2009).
13. J. Y. Kim, M. J. Bae, S. H. Park, T. Jeong, S. Song, J. Lee, I. Han, J. B. Yoo, D. Jung, and S. G. Yu, "Electroluminescence enhancement of the phosphor dispersed in a polymer matrix using the tandem structure," Org. Electron. **12**(3), 529–533 (2011).
14. J. Y. Kim, H. Kim, D. Jung, and S. G. Yu, "Enhanced electroluminescence performances by controlling the position of carbon nanotubes," J. Appl. Phys. **112**(10), 104515 (2012).
15. S. Shinoya, T. Koda, K. Era, and H. Fujiwara, "Nature of luminescence transitions in ZnS crystals," J. Phys. Soc. Jpn. **19**(7), 1157–1167 (1964).
16. K. Manzoor, S. R. Vadera, N. Kumar, and T. R. N. Kutty, "Multicolor electroluminescent devices using doped ZnS nanocrystals," Appl. Phys. Lett. **84**(2), 284–286 (2004).
17. A. G. Fischer, "Electroluminescent lines in ZnS powder particles I," J. Electrochem. Soc. **109**(11), 1043–1049 (1962).
A. G. Fischer, "Electroluminescent lines in ZnS powder particles II," J. Electrochem. Soc. **110**(7), 733–748 (1963).
18. M. I. Abdalla, A. Godin, A. Brenac, and J.-P. Noblanc, "Electrical conduction and degradation mechanisms in powder ZnS:Mn,Cu direct current electroluminescent devices," IEEE Trans. Electron. Dev. **28**(6), 689–693 (1981).
19. B. H. Cumpston and K. F. Jensen, "Electromigration of aluminum cathodes in polymer-based electroluminescent devices," Appl. Phys. Lett. **69**(25), 3941–3943 (1996).
20. K. Hirabayashi, H. Kozawaguchi, and B. Tsujiyama, "Study on A-C powder EL phosphor deterioration factors," J. Electrochem. Soc. **130**(11), 2259–2263 (1983).
21. K. Bhattacharyya, S. M. Goodnick, and J. F. Wager, "Monte Carlo simulation of electron transport in alternating-current thin-film electroluminescent devices," J. Appl. Phys. **73**(7), 3390–3395 (1993).
22. E. Bringuier, "Impact excitation in ZnS-type electroluminescence," J. Appl. Phys. **70**(8), 4505–4512 (1991).
23. D. J. Bergman, "The dielectric constant of a composite material-A problem in classical physics," Phys. Rep. **43**(9), 377–407 (1978).

1. Introduction

The area of flexible and printed electronics (FPE) is currently attracting considerable interest as a means to satisfy future societal needs for smart technology through ubiquitous sensing, computing, and interfacing. Recently, initial applications of FPE are emerging in the fields of display technology [1,2], biomedical devices [3], and energy-harvesting devices [4]. The use of FPE in the lighting sector, however, is relatively rare because of the low luminance efficiency of the devices that results from a lack of proper materials and device structures. The suggested flexible lighting device structures are based on arrays of inorganic light emitting diodes (ILEDs) with flexible interconnects on flexible substrates [1,5]. The fabrication of the device, however, includes rather complex processes such as multilayer deposition, device transfer, and multi-step pattern alignment. In this study, we demonstrate a flexible lighting source based on hybrid structure electroluminescence (HSEL) fabricated by simple process steps at room temperature. A method to improve the luminance efficiency of the device by incorporating highly dielectric composite materials is also validated.

The electroluminescent (EL) device has been used extensively in display and lighting technologies because it has a simple fabrication process and offers a wide viewing angle, large contrast, and fast response [6,7]. Powder EL devices are used for LCD backlights due to their high luminous efficiency while thin film EL (TFEL) devices are primarily used for displays [8]. EL devices often consist of multiple layers with emissive and dielectric layers sandwiched between transparent or reflective electrodes on substrates. The dielectric layer is required to prevent catastrophic breakdown since the device is operated under a high electric field ($>10^6$ V/m) to facilitate the tunneling of charge carriers [9,10]. It also provides a barrier for moisture and ion diffusion. In addition, other physical properties of the dielectric material such as adhesion, optical transparency, and resistance to the thermal or mechanical stress are also important for device operation.

The conventional powder EL device process involves a layer-by-layer deposition of the phosphor and oxide dielectric layer using the screen-printing method [11]. However, the EL

devices fabricated by this technique often suffer from limitations such as poor adhesion and non-uniform layers. Consequently, dielectric breakdown causes the devices to have a short lifetime and the light emission from the device surfaces is not uniform. In order to overcome such limitations, a new device structure consisting of phosphor microparticles embedded within a polymer matrix has been suggested [12–14]. This method simplifies the fabrication steps by forming the emissive regions and dielectric matrix simultaneously. However, since high temperature curing (>120°C) is required to form the polymer matrix, the adhesion between the emissive layer and the electrodes in the devices can weaken because of different thermal expansion between layers. Pinholes can also be easily created in the dielectric layer. Further, the integration of a HSEL device with other devices is difficult due to the thermal damage that occurs during the high temperature curing process.

In this study, we prepared flexible hybrid structure electroluminescent (HSEL) devices by curing a mixture of phosphor powder and pre-polymer with UV irradiation at room temperature. These devices demonstrated a notable improvement in the uniformity of layer thickness and phosphor particle dispersion that resulted in uniform light emission from the surfaces of the HSEL devices. The emissive layer of the devices displayed less pinholes and better adhesion to the electrodes, and consequently the reliability and lifetime of the devices were improved. Furthermore, the luminance of the device was also enhanced more than 200 cd/m^2 when highly dielectric oxide nanoparticles were uniformly dispersed within the polymer matrix.

2. Experimental

Figure 1 displays the schematic diagram of the HSEL device fabrication process. The hybrid phosphor layer was cured by UV irradiation and the light was emitted through both of the top and bottom substrates. A mixture of ZnS:Cu phosphor particles and the pre-polymer was UV-cured after being dispensed between two transparent electrodes. The ZnS:Cu phosphor powder (GGS62, Osram Sylvania) consisted of encapsulated particles with diameters in the range of 20-30 μm. The pre-polymer was composed of a multifunctional dilute (urethane acrylate), a cross-linker monomer, and a photoinitiator. The electrode structure was a transparent conducting oxide (ITO) thin film coated on either a glass substrate or a flexible polyethylene terephthalate (PET) substrate. When UV light was irradiated (1 mW/cm^2, 180 sec) onto the mixture of phosphor powder and pre-polymer, polymers were cross-linked by the reactive radicals released from photoinitiators. Figure 1(b) demonstrates the light emission from a flexible HSEL device. The flexibility of the device originates from the polymer binder matrix and the plastic PET substrate. The HSEL device was bent freely during operation.

The reference polymer binder was composed of 2-ethylhexyl acrylate (EHA, 87 wt%, reactive diluent), CYTEC Ebercryl 810 (10 wt%), 1,6 hexanediol diacrylate (HDDA, 2 wt%), and photoinitiator (1 wt%). In order to develop a highly dielectric polymer binder, various cross-linking monomers were tested for the pre-polymer formulation. The formulation containing 2-hyroxyethyl acrylate (HEA) or 4-hydroxybutyl acrylate (HBA) demonstrated the highest dielectric constants after UV-curing. The formulation of the highly dielectric UV-curable binder used in this work was urethane acrylate (60 wt%): HEA (36 wt%): photoinitiator (4 wt%). To prepare the highly dielectric composite binder, BaTiO$_3$ nanoparticles (Sigma Aldrich) were uniformly dispersed in the pre-polymer solution after treatment in a magnetic stirrer for several hours. To facilitate comparison with the high temperature curing process, a thermally curable binder (α-terpineol: ethyl cellulose = 95:5 wt%) was used for dispersing the phosphor powder. These devices were cured at 120°C for 10 min.
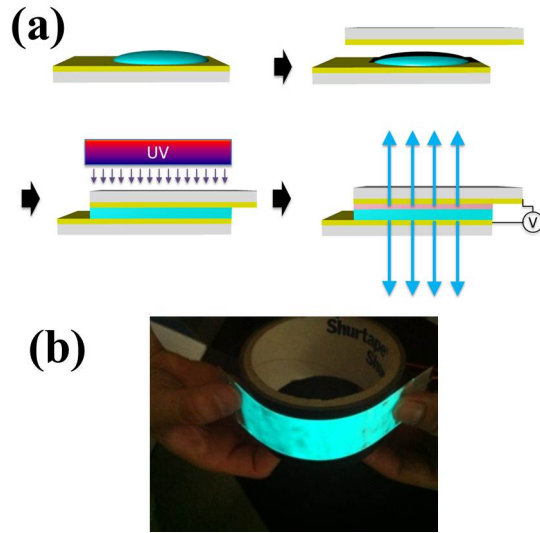
Fig. 1. (a) Schematic diagram of the hybrid structure EL (HSEL) device fabrication process. The hybrid phosphor layer is cured by UV irradiation after the mixture of the ZnS:Cu phosphor particles and the polymer binder is dispensed between two transparent electrodes on a flexible PET or a glass substrate. The light is emitted through both the top and bottom surfaces upon applying ac voltage between two electrodes. (b) Light emission from a flexible HSEL device prepared on transparent plastic substrates.

The cross-sectional topography of the HSEL devices was inspected by high resolution field emission scanning electron microscopy (HR-FESEM SU8020, Hitachi) and the dielectric constant of the binder materials was measured by an impedance analyzer (LCMS-200, Sesim Photonics Tech.) at 20 V and 300 Hz. The luminance of the HSEL devices and CIE 1931 chromaticity coordinate were measured by a spectrometer (CS-1000, Minolta) while applying a sinusoidal alternating current (ac) to the devices.

3. Results and discussion

Figure 2(a) and 2(b) display the SEM cross-section images of the HSEL devices prepared by thermal and UV-curing respectively. The sample in Fig. 2(a) is prepared by dispensing the composite of phosphor and thermally curable polymer binder between two transparent electrodes. The reference polymer binder is used for the sample in Fig. 2(b). As shown in Fig. 2(a), the emissive layer of the thermally cured device has relatively uniform thickness. However, some pinholes or defect lines are created due to the high temperature curing process (>120°C) as indicated in the figure. In contrast, the UV-cured sample in Fig. 2(b) has a uniform cross-section without defects or pinholes. The luminance of the aforementioned device also demonstrates better intensity and uniformity compared to the thermally cured sample as shown in the insets of Fig. 2(a) and 2(b). The emitted light spectrum is in the blue region located at x = 0.15 and y = 0.12 in CIE 1931 chromaticity diagram at 10 kHz and 170 V. The blue emission is associated with the electron traps formed by sulfur vacancies and the emission center formed by Cu-doping in ZnS:Cu phosphor. Following field reversal in the ac EL devices, the trapped electrons are released and radiative recombination with holes occurs [15,16].

Figure 2(c) shows the luminance of EL devices prepared by different fabrication processes. An electric field of 10^6 V/m is typically needed to induce the impact excitation of luminescent dopant centers after the charges trapped at the interface are injected into the conduction band of the phosphor [17]. Therefore, an additional dielectric layer is required for the application of this high voltage. The EL device in which this dielectric layer was

fabricated by the screen-printing process displays high luminance as shown in Fig. 2(c). Surprisingly, in the UV-cured HSEL device, a dielectric layer with approximately 7% of the thickness of the emissive layer was formed between the emissive layer and transparent electrode. This phenomenon may be associated with the UV polymerization process wherein the polymer binder separates from the mixture during the initial polymerization of the top surface of the emissive layer and forms a thin dielectric layer above the emissive layer. The luminance of the UV-cured device at 170 V was approximately 80% of the EL device fabricated by conventional screen-printing. However, in the thermally cured EL device, such dielectric layer formation was difficult causing only a small number of hot electrons to be available to excite the emissive center. Consequently, the luminance of the device was low and quickly saturated above 100 V reaching approximately 50% of the screen-printing device at 170 V as seen in Fig. 2(c).
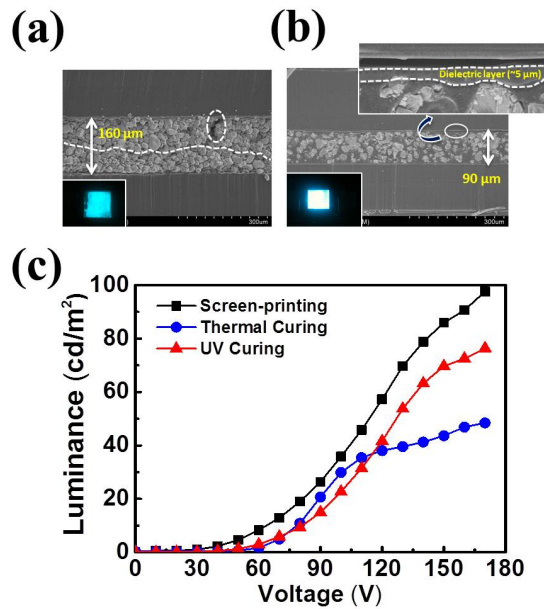

Fig. 2. SEM cross-section images of the HSEL devices prepared by (a) thermal and (b) UV-curing of the mixture of phosphor powder and polymer binder. Both of the samples are prepared on ITO coated PET substrates. In the emissive layer, ZnS:Cu phosphor particles are dispersed within a polymer matrix. A defect line and a pinhole created after thermal curing are shown in (a). The top inset in (b) displays a dielectric layer formed after UV-curing. The bottom insets exhibit the optical images of the operating HSEL device. (c) Luminance vs. applied voltage (10 kHz) of HSEL devices prepared by different processes (i.e. screen-printing, thermal curing, and UV-curing)

In the optical image of the operating HSEL devices, black spots are shown in some regions on the surfaces. Such degradation of EL devices is known to be caused by non-uniform thickness of dielectric layer, dopant migration [18], metal migration from electrodes [19], and sulfur migration due to moisture. However, we believe that the degradation by dopant migration or metal migration from electrodes is negligible since our device is operated by an alternating electric field. When the counter electrodes are not strongly insulated by dielectric materials, black spots can form due to dielectric breakdown. In addition, the non-uniformity of the dielectric thickness causes a non-uniform electric field to be formed when current is applied to the devices. Under this condition, defects can be easily formed and dielectric loss can occur. Consequently, the non-uniformity in the dielectric layer affects the long term reliability of the EL devices. Defects in this layer also inhibit its ability to function

as a barrier to moisture and ion diffusion. When a phosphor interacts with moisture, a sulfur molecule is lost due to the following reaction [20]

$$ZnS + 2H_2O \rightarrow SO_2 + Zn + 2H_2. \tag{1}$$

Through reaction with moisture, ZnS loses its crystallinity because of an increase in Zn and S vacancies and the generated gases degrade the EL device by separating layers or interfaces. For the HSEL devices, in addition to the encapsulation to the ZnS:Cu phosphor particles, the polymer binder containing urethane acrylate further prevents moisture from degrading the phosphor particles.
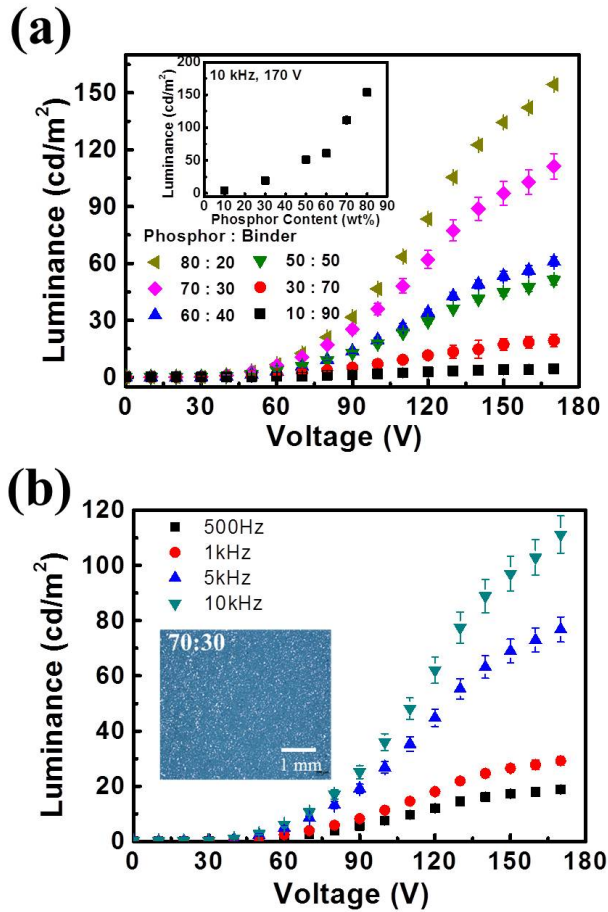

Fig. 3. (a) Luminance vs. applied ac voltage (10 kHz) for different wt% ratios of the phosphor and polymer binder. The inset illustrates the dependence of the luminance on the phosphor contents at 10 kHz and 170 V. (b) Luminance vs. applied ac voltage for different frequencies. The mixing ratio of ZnS:Cu phosphor and polymer binder is 70:30 wt%. The inset shows the surface topography of the HSEL device.

In order to optimize the mixing ratio between phosphor and polymer binder, we investigated the dependence of the luminance of HSEL devices on the content of the phosphor particles in the emissive layer. In this experiment, we used a highly dielectric UV-curable pre-polymer formulation. The measured dielectric constant of this material at 20 V and 300 Hz was 17.2. As shown in Fig. 3(a), the luminance increases as the phosphor content increases. Since the density of the emissive center increases, the luminance is highest for the device with

largest amount of phosphors. However, the small amount of polymer binder used for the 80:20 wt% sample caused fabrication problems such as poor adhesion between layers and non-uniform luminance. Therefore, the optimal mixing ratio between phosphors and polymer binder is 70:30 wt%, and the maximum luminance of the device is 111 cd/m^2 at 10 kHz and 170 V. The luminance is increased by 46% compared to the device with the reference polymer binder operating under the same conditions (76 cd/m^2). Figure 3(b) illustrates the frequency dependence of the luminance for the 70:30 wt% sample. The luminance intensity increases and slowly saturates with the applied voltage and frequency. This observed increase is the result of an increase in scattering and the scattering rate at higher frequencies [21,22]. The frequency of the applied voltage is fixed at 10 kHz in this study.
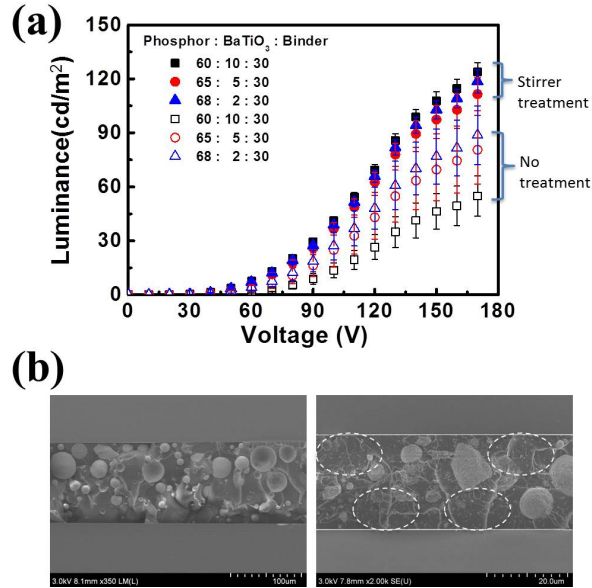

Fig. 4. (a) Luminance vs. applied ac voltage (10 kHz) for HSEL devices with different formulations of the emitting layer. The weight ratio between the phosphor and BTO particles is varied while the content of the polymer binder is fixed at 30 wt%. The open and solid symbols correspond to the samples without and with BTO dispersion treatment respectively. (b) SEM cross-section images of the UV-cured mixture of BTO powder and polymer binder without (left) and with (right) dispersion treatment. The mixing ratio of BTO powder and polymer binder is 1:2 by weight. The circled regions indicate BTO nanoparticles dispersed in the polymer matrix.

Although the concept of using highly dielectric UV-curable polymer binder in a HSEL device was successful, the luminance of the device was still not sufficient to enable the device to be used as a commercial product. In order to further improve the luminance of the HSEL device, we considered mixing highly dielectric BaTiO$_3$ (BTO) nanoparticles ($\varepsilon = 150$) with the pre-polymer. Figure 4(a) displays the luminance properties of HSEL devices with different amounts of BTO nanoparticles. In this instance, the content of polymer binder is fixed at 30 wt% in order to investigate the effect of the oxide nanoparticles on the luminance of the HSEL devices. Without dispersion treatment of oxide nanoparticles (open symbols), the enhancement of the luminance is not observed because the higher BTO content did not improve the luminance of the HSEL device. The luminance of the EL devices is improved only when the oxide nanoparticles were uniformly dispersed in the polymer binder (solid symbols). To facilitate uniform particle dispersion, the BTO powder was dispersed in ethanol and the resulting solution was treated with a magnetic stirrer for several hours. Then the nanoparticles were dried in an oven prior to being mixed with the pre-polymer. Following

dispersion treatment, the luminance of the HSEL devices greatly improved. For example, utilizing the same mixing ratio of 60:10:30 wt%, the device luminance is 124 cd/m^2 after dispersion treatment while it is only 55 cd/m^2 before dispersion treatment. In order to clarify the effect of dispersion treatment, SEM cross-sectional images of the UV-cured mixture of BTO powder and polymer binder (1:2 by weight) were taken and are shown in Fig. 4(b). Compared to the untreated sample, the stirrer treatment uniformly disperses BTO nanoparticles between the micron-sized particles in the polymer matrix as indicated by the circles in the right panel. Using a highly dielectric binder material is very important for the luminance efficiency of an EL device. For example, the electric field applied to the phosphor of a TFEL device

$$E_p = \frac{\varepsilon_d}{\varepsilon_d L_p + \varepsilon_p L_d} V \tag{2}$$

where ε_d and ε_p are the permittivity of the dielectric and the phosphor layer respectively, and L_d and L_p are the thickness of each of the layers [8,10]. In order to have a high electric field applied to the phosphor layers, ε_d should be large and the emitting layer should be thin. For HSEL devices, the effective dielectric constant of the composite material can be increased when the BTO nanoparticles are uniformly dispersed in the polymer matrix [23]. In addition, the alternating external electric field can be effectively enhanced near the highly dielectric oxide nanoparticles in the polymer matrix, thus the trapped charges at the interfaces and defects can have a higher probability of tunneling through the potential barrier to excite emissive centers in the phosphor particles.
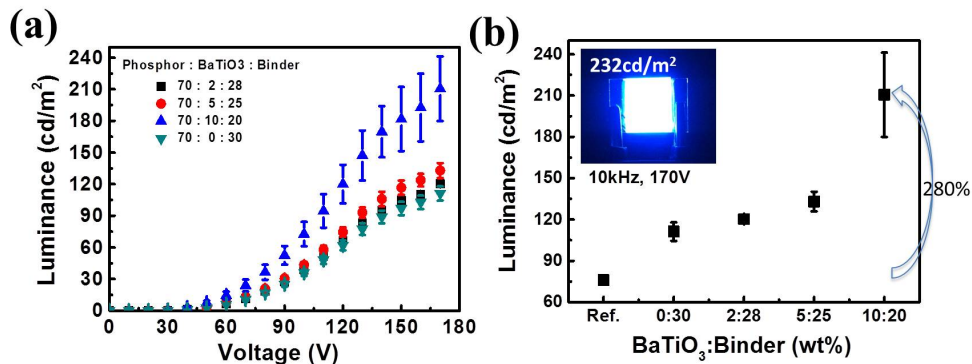

Fig. 5. (a) Luminance vs. applied ac voltage (10 kHz) for the HSEL devices with different formulations of the emitting layer. The weight ratio between the polymer binder and the BTO powder is varied while the content of the phosphor is fixed at 70 wt%. (b) Luminance of HSEL devices vs. oxide-polymer composite with different mixing ratio (wt%). The devices are operated under the same condition at 10 kHz and 170 V. The average luminance of a HSEL device with the highest oxide content was up to 211 cd/m^2, which is approximately a 280% increase compared to the HSEL device with the reference polymer binder without oxide nanoparticles. The inset displays the optical image of the operating HSEL device with a maximum luminance of 232 cd/m^2.

Figure 5(a) displays the luminance of HSEL devices with different formulations of the emitting layer. The weight ratio between the polymer binder and the BTO is varied while the content of the phosphor is fixed at 70 wt%. The luminance increases considerably as the content of BTO nanoparticles in the polymer binder is increased. Figure 5(b) summarizes the result of the HSEL devices with different contents of the oxide-polymer composite. For the same phosphor contents of 70 wt%, we could obtain luminance up to 111 cd/m^2 using a highly dielectric UV-curable polymer binder compared to 76 cd/m^2 of the sample with the reference polymer binder. The luminance further improves up to 211 cd/m^2 on average by

uniformly dispersing BTO nanoparticles within the polymer matrix. The luminance of HSEL devices containing the highly dielectric composite increase approximately 280% compared to those devices containing the reference polymer binder without oxide nanoparticles. The inset figure displays the operating HSEL device with the oxide-polymer composite binder that demonstrated a maximum luminance of 232 cd/m^2. Our study demonstrates a pathway to highly efficient, flexible EL devices that can also potentially be applied to flexible and printed electronic signs, displays, and lighting in the future.

4. Conclusion

In conclusion, generating an efficient EL device utilizing suitable insulating materials and fabrication processes is not a facile task because the insulating layer or matrix should have a high dielectric constant, uniform thickness, and no pinholes. Using a highly dielectric UV-curable polymer binder, we were able to create a flexible HSEL device by a simple fabrication process. We observed a maximum luminance of 111 cd/m^2 at 10 kHz and 170 V by the optimizing the mixing ratio between the phosphor and the polymer binder. Furthermore, by uniformly dispersing highly dielectric BTO nanoparticles within the polymer matrix, we were able to increase the luminance up to 211 cd/m^2 without losing device integrity. This process greatly simplifies the steps required to fabricate powder EL devices by simultaneously forming the emissive regions in the dielectric matrix at room temperature. This work also demonstrates a pathway for creating flexible and printed light emitting devices in the future.